# Supporting Information: Polariton Ring Currents and Circular Dichroism Signals of Mg-porphyrin in a Chiral Cavity

Shichao Sun, Bing Gu, and Shaul Mukamel*

*Department of Chemistry and Department of Physics & Astronomy, University of California, Irvine*

E-mail: smukamel@uci.edu

## Contents

# 1 Chiral Cavities made with Faraday Rotator or Chiral Mirrors

In an ordinary (Fabry-Perit) cavity, a circularly polarized light ($\mathbf{E}^{FP}_{\mathrm{in},\pm} = i\sqrt{\frac{\hbar\omega_c}{2V\epsilon_0}}[\mathbf{e}_\pm e^{i(\mathbf{k}\cdot\mathbf{r}-\omega t)} - \mathbf{e}_\mp e^{-i(\mathbf{k}\cdot\mathbf{r}-\omega t)}]$ reflected by a normal mirror has an opposite circular polarization and propagation direction ($\mathbf{E}^{FP}_{\mathrm{re},\pm} = i\sqrt{\frac{\hbar\omega_c}{2V\epsilon_0}}[\mathbf{e}_\pm e^{i(-\mathbf{k}\cdot\mathbf{r}-\omega t)} - \mathbf{e}_\mp e^{-i(-\mathbf{k}\cdot\mathbf{r}-\omega t)}]$), thus forming a circularly polarized standing wave ($\mathbf{E}^{FP}_{\mathrm{st},\pm} = 2\sqrt{2}\sqrt{\frac{\hbar\omega_c}{2V\epsilon_0}}\cos(\mathbf{k}\cdot\mathbf{r})[\mathbf{e}_x\sin(\omega t) \mp \mathbf{e}_y\cos(\omega t)]$). Note that replacing $t$ with $-t$ makes $\mathbf{E}^{FP}_{\mathrm{st},+}$ become equivalent to $\mathbf{E}^{FP}_{\mathrm{st},+}$ and vice versa. Thus, for a cavity with time reversal symmetry, these two modes with different circular polarization coexist and make the cavity achiral.

In a chiral cavity made with Faraday rotator, the incoming wave with different circular polarization

$$\begin{aligned}\mathbf{E}^{Faraday}_{\mathrm{in},\,+} &= i\sqrt{\frac{\hbar\omega_c}{2V\epsilon_0}}[\mathbf{e}_+ e^{i(\mathbf{k}\cdot\mathbf{r}-\omega t)} - \mathbf{e}_- e^{-i(\mathbf{k}\cdot\mathbf{r}-\omega t)}]\\ \mathbf{E}^{Faraday}_{\mathrm{in},\,-} &= i\sqrt{\frac{\hbar\omega_c}{2V\epsilon_0}}[\mathbf{e}_- e^{i(\mathbf{k}\cdot\mathbf{r}-\omega t)} - \mathbf{e}_+ e^{-i(\mathbf{k}\cdot\mathbf{r}-\omega t)}]\end{aligned} \tag{S1}$$

reflected by Faraday mirror, results in the reflected wave

$$\begin{aligned}\mathbf{E}^{Faraday}_{\mathrm{re},\,+} &= i\sqrt{\frac{\hbar\omega_c}{2V\epsilon_0}}[\mathbf{e}_+ e^{i(-\mathbf{k}\cdot\mathbf{r}-\omega t+\varphi)} - \mathbf{e}_- e^{-i(-\mathbf{k}\cdot\mathbf{r}-\omega t+\varphi)}]\\ \mathbf{E}^{Faraday}_{\mathrm{re},\,-} &= i\sqrt{\frac{\hbar\omega_c}{2V\epsilon_0}}[\mathbf{e}_- e^{i(-\mathbf{k}\cdot\mathbf{r}-\omega t-\varphi)} - \mathbf{e}_+ e^{-i(-\mathbf{k}\cdot\mathbf{r}-\omega t-\varphi)}]\end{aligned} \tag{S2}$$

where $\pm\varphi$ is the phase shift caused by the Faraday rotator. The incoming wave and reflected wave form standing wave

$$\begin{aligned}\mathbf{E}^{Faraday}_{\mathrm{st},\,+} &= 2\sqrt{2}\sqrt{\frac{\hbar\omega_c}{2V\epsilon_0}}\cos(\mathbf{k}\cdot\mathbf{r}-\frac{\varphi}{2})[\mathbf{e}_x\sin(\omega t-\frac{\varphi}{2}) - \mathbf{e}_y\cos(\omega t-\frac{\varphi}{2})]\\ \mathbf{E}^{Faraday}_{\mathrm{st},\,-} &= 2\sqrt{2}\sqrt{\frac{\hbar\omega_c}{2V\epsilon_0}}\cos(\mathbf{k}\cdot\mathbf{r}+\frac{\varphi}{2})[\mathbf{e}_x\sin(\omega t+\frac{\varphi}{2}) + \mathbf{e}_y\cos(\omega t+\frac{\varphi}{2})]\end{aligned} \tag{S3}$$

The spatial envelope of the standing wave with different circular polarization is $E^{Faraday}_{\text{envelope},\pm}(r) = \cos(\mathbf{k}\cdot\mathbf{r} \mp \frac{\varphi}{2})$. The phase difference of the envelope with different polarization can be tuned through changing the thickness of the Faraday rotator and the magnetic field strength applied on the Faraday rotator.

If we only consider the field at the peak of right circularly polarized standing wave, in quantized form, the incoming light is

$$\mathbf{E}_{\text{in}} = i\sqrt{\frac{\hbar\omega_c}{2V\epsilon_0}}[\mathbf{e}_+ a e^{i(k\cdot r-\omega t)} - \mathbf{e}_- a^\dagger e^{-i(k\cdot r-\omega t)}] \tag{S4}$$

and the reflected light

$$\mathbf{E}_{\text{re}} = i\sqrt{\frac{\hbar\omega_c}{2V\epsilon_0}}[\mathbf{e}_+ a e^{i(-k\cdot r-\omega t)} - \mathbf{e}_- a^\dagger e^{-i(-k\cdot r-\omega t)}] \tag{S5}$$

combining Eq. (S4) and Eq. (S5), we obtain the quantized circularly polarized standing wave Eq. (3) in the main text.

The other type of chiral cavities is composed with chiral mirrors.[S1,S2] For this cavity, the wave reflected by a chiral mirror is $\mathbf{E}_{\text{re},\pm} = i\sqrt{\frac{\hbar\omega_c}{2V\epsilon_0}}[\mathbf{e}_\mp e^{i(-\mathbf{k}\cdot\mathbf{r}-\omega t)} - \mathbf{e}_\pm e^{-i(-\mathbf{k}\cdot\mathbf{r}-\omega t)}]$, which combines with the incoming wave $\mathbf{E}_{\text{in},\pm} = i\sqrt{\frac{\hbar\omega_c}{2V\epsilon_0}}[\mathbf{e}_\pm e^{i(\mathbf{k}\cdot\mathbf{r}-\omega t)} - \mathbf{e}_\mp e^{-i(\mathbf{k}\cdot\mathbf{r}-\omega t)}]$ to form a standing wave $\mathbf{E}_{\text{st},\pm} = -2\sqrt{2}\sqrt{\frac{\hbar\omega_c}{2V\epsilon_0}}\cos(\omega t)[\mathbf{e}_x\cos(\mathbf{k}\cdot\mathbf{r}) \mp \mathbf{e}_y\sin(\mathbf{k}\cdot\mathbf{r})]$. The standing wave polarization at a position does not rotate with time, but the polarization changes with the spatial coordinate. For a molecule whose size is small compared with the wavelength of the cavity mode, at a fixed position, it only feels linear polarization in a helical cavity. However, when the wavelength of the cavity mode is comparable with molecular size, for example, a molecule in an X-ray cavity, or a polymer in an optical cavity with the chain aligned perpendicular to the mirror, the molecule can feel the helical polarization in the chiral cavity made with chiral mirrors.

## 2 Chiral Cavity

A chiral cavity can be constructed with Faraday rotators.[S2] As schematically shown in Fig. 1 of the main text, the chiral optical cavity can be built with two parallel Faraday mirrors, where each mirror is composed of a regular mirror and a Faraday rotator.[S2] The magnetic field can be applied along either direction of the cavity axis (+x and -x) such that the rotation angle in the polarization induced by the two Faraday rotators does not cancel.

To design a chiral cavity, the Faraday rotation can be achieved by combining the strong magnetic field with a Faraday rotator with large Verdet constant in UV-visible region. For the chiral cavity in this work with resonant frequency $\omega_c$ = 2.44 eV (corresponding to 509 nm), the distance between mirrors is approximately 10 µm. With the magnetic field of 45 T[S3] and the Faraday rotator RuTPP[S4] with thickness of approximately 4000 nm, the standing wave of 509 nm can be rotated by 90 degrees. Such Faraday rotator can be fitted into an optical micro-cavity.

## 3 State to State Transition Electric Dipole of Mg-Porphyrin

The molecular excited state energy and the transition dipole from ground state to excited states of Mg-porphyrin molecule with Tamm-Dancoff approximation are displayed in Tab. S1

**Table S1.** Energies and transition dipoles of molecular excited states. The transition electric dipoles $\langle g|\boldsymbol{\mu}|e\rangle$ are in atomic units.

| state | irreducible representation | energy (eV) | $\langle g\|\mu_x\|e\rangle$ | $\langle g\|\mu_y\|e\rangle$ | $\langle g\|\mu_z\|e\rangle$ |
|---|---|---|---|---|---|
| 1 | $E_u$ | 2.4481 | 0.0000 | 0.0000 | 0.1497 |
| 2 | $E_u$ | 2.4481 | 0.0000 | −0.1494 | 0.0000 |
| 3 | - | 3.7959 | 0.0000 | 0.0000 | 0.0000 |
| 4 | $E_u$ | 3.8056 | 0.0000 | −1.1176 | 0.0000 |
| 5 | $E_u$ | 3.8056 | 0.0000 | 0.0000 | −1.1184 |
| 6 | - | 3.8527 | 0.0000 | 0.0000 | 0.0000 |
| 7 | - | 3.9845 | 0.0000 | 0.0000 | 0.0000 |
| 8 | $E_u$ | 4.0601 | 0.0000 | 2.6468 | 0.0000 |
| 9 | $E_u$ | 4.0601 | 0.0000 | 0.0000 | −2.6470 |
| 10 | - | 4.0926 | 0.0000 | 0.0000 | 0.0000 |

The molecular excited state to excited state transition electric dipole of Mg-porphyrin molecule calculated with Tamm-Dancoff approximation is displayed in Tab. S2.

**Table S2.** State to State Transition Electric Dipole of Mg-Porphyrin The transition electric dipoles $\langle e_1|\boldsymbol{\mu}|e_2\rangle$ are in atomic unit $ea_0$.

| state $e_1$ | state $e_2$ | $\langle e_1\|\mu_x\|e_2\rangle$ | $\langle e_1\|\mu_y\|e_2\rangle$ | $\langle e_1\|\mu_z\|e_2\rangle$ |
|---|---|---|---|---|
| 2 | 1 | 0.0000 | 0.0000 | 0.0000 |
| 3 | 1 | 0.0000 | -1.1731 | 0.0000 |
| 3 | 2 | 0.0000 | 0.0000 | -1.1730 |
| 4 | 1 | 0.0000 | 0.0000 | 0.0000 |
| 4 | 2 | 0.0000 | 0.0000 | 0.0000 |
| 4 | 3 | 0.0000 | 0.0000 | 2.7550 |
| 5 | 1 | 0.0000 | 0.0000 | 0.0000 |
| 5 | 2 | 0.0000 | 0.0000 | 0.0000 |
| 5 | 3 | 0.0000 | -2.7467 | 0.0000 |
| 5 | 4 | 0.0000 | 0.0000 | 0.0000 |
| 6 | 1 | 0.0000 | -0.1479 | 0.0000 |
| 6 | 2 | 0.0000 | 0.0000 | 0.1509 |
| 6 | 3 | 0.0000 | 0.0000 | 0.0000 |
| 6 | 4 | 0.0000 | 0.0000 | 3.5669 |
| 6 | 5 | 0.0000 | 3.5729 | 0.0000 |
| 7 | 1 | 0.0000 | 0.0000 | 0.1343 |
| 7 | 2 | 0.0000 | 0.1346 | 0.0000 |
| 7 | 3 | 0.0000 | 0.0000 | 0.0000 |
| 7 | 4 | 0.0000 | 1.8826 | 0.0000 |
| 7 | 5 | 0.0000 | 0.0000 | -1.8806 |
| 7 | 6 | 0.0000 | 0.0000 | 0.0000 |
| 8 | 1 | 0.0000 | 0.0000 | 0.0000 |
| 8 | 2 | 0.0000 | 0.0000 | 0.0000 |
| 8 | 3 | 0.0000 | 0.0000 | -0.5440 |
| 8 | 4 | 0.0000 | 0.0000 | 0.0000 |
| 8 | 5 | 0.0000 | 0.0000 | 0.0000 |
| 8 | 6 | 0.0000 | 0.0000 | -0.7054 |
| 8 | 7 | 0.0000 | 3.3795 | 0.0000 |
| 9 | 1 | 0.0000 | 0.0000 | 0.0000 |
| 9 | 2 | 0.0000 | 0.0000 | 0.0000 |
| 9 | 3 | 0.0000 | -0.5418 | 0.0000 |
| 9 | 4 | 0.0000 | 0.0000 | 0.0000 |
| 9 | 5 | 0.0000 | 0.0000 | 0.0000 |

| | | | | |
|---|---|---|---|---|
| 9 | 6 | 0.0000 | 0.7059 | 0.0000 |
| 9 | 7 | 0.0000 | 0.0000 | 3.3775 |
| 9 | 8 | 0.0000 | 0.0000 | 0.0000 |
| 10 | 1 | 0.0000 | 0.0000 | -0.0605 |
| 10 | 2 | 0.0000 | 0.0607 | 0.0000 |
| 10 | 3 | 0.0000 | 0.0000 | 0.0000 |
| 10 | 4 | 0.0000 | 2.5231 | 0.0000 |
| 10 | 5 | 0.0000 | 0.0000 | 2.5248 |
| 10 | 6 | 0.0000 | 0.0000 | 0.0000 |
| 10 | 7 | 0.0000 | 0.0000 | 0.0000 |
| 10 | 8 | 0.0000 | 2.7625 | 0.0000 |
| 10 | 9 | 0.0000 | 0.0000 | -2.7653 |

# 4 Legend of Figure 13

Here we give the legend for Fig. 13 in the maintext in Fig. S1.

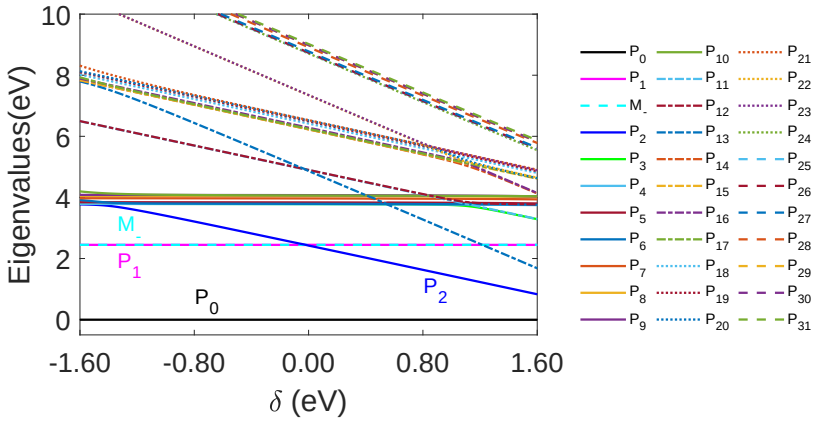


**Figure S1.** Polariton energy variation with detuning for coupling strength $g = 1.028 \times 10^{-1}$ V/Å.

# 5 Excited States of Mg-Porphyrin in the Magnetic Field

Mg-porphyrin molecular excited state energies and ground state to excited state transition electric dipoles in the magnetic field are displayed in Tab. S3. The energies and transition electric dipoles are calculated with complex linear-response TDDFT with B3LYP functional and gaussian type orbital 6-31g(d) in Chronus quantum.[S5–S7]

**Table S3.** Energies and transition electric dipoles of Mg-porphyrin molecular excited states in the magnetic field. The transition electric dipoles $\langle g|\boldsymbol{\mu}|e\rangle$ are in atomic units $ea_0$.

| state | energy(eV) | $\langle g\|\mu_x\|e\rangle$ | $\langle g\|\mu_y\|e\rangle$ | $\langle g\|\mu_z\|e\rangle$ |
|---|---|---|---|---|
| 1 | 2.38469715 | 0.0000 | $-0.0728423 - i0.00416749$ | $0.00418285 - i0.0731107$ |
| 2 | 2.38981000 | 0.0000 | $-0.0426288e - i0.0588642$ | $-0.0590594 + i0.0427701$ |
| 3 | 3.51556535 | 0.0000 | $1.85717 + i1.31835$ | $0.537895 - i2.23061$ |
| 4 | 3.51600720 | 0.0000 | $-0.785631 - i2.15668$ | $-2.14083 + i0.779860$ |
| 5 | 3.75266770 | 0.0000 | 0.0000 | 0.0000 |
| 6 | 3.78367354 | 0.0000 | $0.140460 - i0.573901$ | $-0.541453 - i0.132519$ |
| 7 | 3.78618445 | 0.0000 | $-0.143369 - i0.535786$ | $0.567937 - i0.151972$ |
| 8 | 3.79667661 | 0.0000 | 0.0000 | 0.0000 |
| 9 | 3.92726843 | 0.0000 | 0.0000 | 0.0000 |
| 10 | 4.00832131 | 0.0000 | 0.0000 | 0.0000 |
| 11 | 4.11241994 | 0.0000 | 0.0000 | 0.0000 |
| 12 | 4.23749969 | 0.0000 | $0.242406 + i1.05774$ | $-1.00968 + i0.231392$ |
| 13 | 4.23981572 | 0.0000 | $-0.909431 - i0.490319$ | $-0.513785 + i0.952955$ |
| 14 | 4.24959789 | 0.0000 | 0.0000 | 0.0000 |

# References


(S1) Plum, E.; Zheludev, N. I. Chiral Mirrors. *Appl. Phys. Lett.* **2015**, *106*, 221901.

(S2) Hübener, H.; De Giovannini, U.; Schäfer, C.; Andberger, J.; Ruggenthaler, M.; Faist, J.; Rubio, A. Engineering quantum materials with chiral optical cavities. *Nat. Mater.* **2021**, *20*, 438–442.

(S3) Kudisch, B.; Maiuri, M.; Moretti, L.; Oviedo, M. B.; Wang, L.; Oblinsky, D. G.; Prud'homme, R. K.; Wong, B. M.; McGill, S. A.; Scholes, G. D. Ring currents modulate

optoelectronic properties of aromatic chromophores at 25 T. *Proc. Natl. Acad. Sci. U.S.A.* **2020**, *117*, 11289–11298.

(S4) Nelson, Z.; Delage-Laurin, L.; Peeks, M. D.; Swager, T. M. Large Faraday Rotation in Optical-Quality Phthalocyanine and Porphyrin Thin Films. *J. Am. Chem. Soc.* **2021**, *143*, 7096–7103, PMID: 33905654.

(S5) Sun, S.; Williams-Young, D.; Li, X. An Ab Initio Linear Response Method for Computing Magnetic Circular Dichroism Spectra with Nonperturbative Treatment of Magnetic Field. *J. Chem. Theory Comput.* **2019**, *15*, 3162–3169.

(S6) Sun, S.; Beck, R.; Williams-Young, D. B.; Li, X. Simulating Magnetic Circular Dichroism Spectra with Real-Time Time-Dependent Density Functional Theory in Gauge Including Atomic Orbitals. *J. Chem. Theory Comput.* **2019**, *15*, 6824–6831.

(S7) Sun, S.; Li, X. Relativistic Effects in Magnetic Circular Dichroism: Restricted Magnetic Balance and Temperature Dependence. *J. Chem. Theory Comput.* **2020**, *16*, 4533–4542.